Repeated Contrast-Enhanced Micro-CT Examinations Decrease Animal Welfare and Influence Tumor Physiology

Jasmin Baier, MSc, Anne Rix, MSc,* Milita Darguzyte, PhD,* Renée Michèle Girbig, MSc,* Jan-Niklas May, MSc,* Rupert Palme, DVM,† René Tolba, MD,‡ and Fabian Kiessling, MD**

Objectives: Computed tomography (CT) imaging is considered relatively safe and is often used in preclinical research to study physiological processes. However, the sum of low-dose radiation, anesthesia, and animal handling might impact animal welfare and physiological parameters. This is particularly relevant for longitudinal studies with repeated CT examinations. Therefore, we investigated the influence of repeated native and contrast-enhanced (CE) CT on animal welfare and tumor physiology in regorafenib-treated and nontreated tumor-bearing mice.

Material and Methods: Mice bearing 4T1 breast cancer were divided into 5 groups: (1) no imaging, (2) isoflurane anesthesia only, (3) 4 mGy CT, (4) 50 mGy CT, and (5) CE-CT (iomeprol). In addition, half of each group was treated with the multikinase inhibitor regorafenib. Mice were imaged 3 times within 1 week under isoflurane anesthesia. Behavioral alterations were investigated by score sheet evaluation, rotarod test, heart rate measurements, and fecal corticosterone metabolite analysis. Tumor growth was measured daily with a caliper. Tumors were excised at the end of the experiment and histologically examined for blood vessel density, perfusion, and cell proliferation.

Results: According to the score sheet, animals showed a higher burden after anesthesia administration and in addition with CT imaging ($P < 0.001$). Motor coordination was not affected by native CT, but significantly decreased after CE-CT in combination with the tumor therapy ($P < 0.001$). Whereas tumor growth and blood vessel density were not influenced by anesthesia or imaging, CT-scanned animals had a higher tumor perfusion ($P < 0.001$) and a lower tumor cell proliferation ($P < 0.001$) for both radiation doses. The most significant difference was observed between the control and CE-CT groups.

Conclusion: Repeated (CE-) CT imaging of anesthetized animals can lead to an impairment of animal motor coordination and, thus, welfare. Furthermore, these standard CT protocols seem to be capable of inducing alterations in tumor physiology when applied repetitively. These potential effects of native and CE-CT should be carefully considered in preclinical oncological research.

Key Words: CT, animal welfare, severity assessment, long-term effects, regorafenib, isoflurane, anesthesia, behavior, rotarod, breast cancer, low-dose, iomeprol

(*Invest Radiol* 2023;58: 00–00)

Received for publication August 17, 2022; and accepted for publication, after revision, October 2, 2022.

From the *Institute for Experimental Molecular Imaging, Medical Faculty, RWTH Aachen International University, Aachen, Germany; †Department of Biomedical Sciences, University of Veterinary Medicine Vienna, Vienna, Austria; and ‡Institute for Laboratory Animal Science and Experimental Surgery, Medical Faculty, RWTH Aachen International University, Aachen, Germany.

Conflicts of interest and sources of funding: This research was funded by the Deutsche Forschungsgemeinschaft (DFG) project number 321137804 and the DFG research training group RTG 2375: project number: 331065168.

Institute address: Institute for Experimental Molecular Imaging, Center for Biohybrid Medical Systems, Forckenbeckstrasse 55, 52074 Aachen, Germany.

Correspondence to: Fabian Kiessling, MD, Institute for Experimental Molecular Imaging, Center for Biohybrid Medical Systems, Forckenbeckstrasse 55, 52074 Aachen, Germany. E-mail: fkiessling@ukaachen.de.

Supplemental digital contents are available for this article. Direct URL citations appear in the printed text and are provided in the HTML and PDF versions of this article on the journal's Web site (www.investigativeradiology.com).

ISSN: 0020-9996/23/5805–0000
DOI: 10.1097/RLI.0000000000000936

Preclinical research underlays the ethical imperative to minimize animal burden by considering the 3Rs.[1] This concept was first introduced by Russel and Burch in 1959 and stands for reduction, replacement, and refinement of animal experiments. One regularly used tool to investigate physiological and morphological processes in preclinical research is noninvasive imaging.[2,3] With regard to the 3Rs, imaging contributes significantly to the reduction of animal numbers required for a study by enabling longitudinal scans of the same animal.[4] Whereas it was shown that, for example, magnetic resonance imaging and ultrasound imaging are well tolerated by animals and highly suited for preclinical research,[5,6] other modalities have not yet profoundly been explored concerning risks and possible unwanted side effects on animal well-being and study results.

Imaging procedures often require the intravenous administration of contrast agents, and even if these are approved for clinical use, their repeated administration in short periods may compromise animal welfare and physiological parameters. In this context, it has been shown that linear gadolinium-based contrast agents for magnetic resonance imaging have high retention in the brain and, moreover, can lead to nephrogenic systemic fibrosis in patients.[7] Furthermore, the most commonly used contrast agents for computed tomography (CT) imaging are iodine based[8] and have mainly shown side effects such as allergic reactions, nephrotoxicity,[9] or alterations in liver enzymes.[10] In addition, a correlation between DNA strand breakage[11] and the use of iodine contrast agents as well as alterations in blood parameters[10] were demonstrated in preclinical studies.

Besides contrast agent applications, a common element of all preclinical imaging studies is the administration of anesthesia to immobilize the animals during the procedure. Apart from the high risk of hypothermia and hypoglycemia during the anesthesia, the administration can lead to a long-term alteration of physiological parameters, resulting in unintended changes in the experimental results.[12] The most commonly used general anesthetics are injectable agents, such as pentobarbital and ketamine, or inhalation agents, such as isoflurane, sevoflurane, and halothane.[12] Both groups of anesthetics can have side effects like immune response alterations,[13,14] as well as mutagenic and hepatotoxic reactions.[12] In addition, the handling itself can increase the stress levels of the animals[15] by inducing changes in the body temperature, central blood pressure, and heart rate.[16] Consequently, psychological and physical stress can lead to alterations in immune responses.[17]

One commonly used imaging modality in preclinical and clinical diagnostics is x-ray CT.[18] Modern devices require much lower radiation doses than in the past[19] and clinical standard protocols typically result in radiation exposure within a dose range of 2 mGy[20] to 100 mGy,[21] which is considered acceptable for patients.[22] However, the effects and risks of these radiation exposures and absorbed dosages in preclinical animal studies can differ tremendously from clinical setups and are often not comparable with patient studies.[21]

Previous preclinical studies have shown that possible effects caused by radiation increase with scan frequency and higher radiation dosages.[23] Especially in preclinical monitoring studies, scans are often performed in a short interval, which can lead to an accumulation of radiation dose over time and, therefore, might affect animal

behavior and study outcome. At low irradiation doses, contradictory results can be found in the literature about the possible influence on animal behavior. Whereas a study by Pecaut et al[24] revealed that neither rotarod performance nor open field exploratory behavior of C57BL/6 mice was affected after single irradiation with doses between 100 mGy and 2 Gy, Giarola et al[25] observed changes in anxiety-related behavior in rats offspring after 1-time radiation with 15 mGy. At higher doses, reports of possible behavioral changes become more frequent. A study with a radiation dosage of 245 mGy showed that selective radiation of the brain causes changes in rats' exploratory behavior and overall activity.[26] Furthermore, Poojary and colleagues[27] reported a tremendous decrease in rotarod performance in Swiss albino mice after 1-time radiation at 5 Gy.

In addition to alterations in animal behavior, various physiological reactions were reported after low-dose radiation ranging from genetic and epigenetic changes to immunological alterations and tumorigenesis.[21] In a study by MacCallum et al,[28] low-dose radiation of 10 mGy was shown to induce DNA damage by Trp53 pathway upregulation after only 1 time of imaging. Furthermore, a decrease in hypoxia-related erythropoietin and vascular endothelial growth factor receptor expression in S180 sarcoma was found after x-ray radiation with 75 mGy.[29]

Although individual procedures might not have an adverse effect on animal welfare, an accumulation of interventions can potentially lead to an impact on animal welfare and, moreover, physiological parameters. To our knowledge, no systematic study has been conducted yet investigating the possible influence of repeated diagnostic CT imaging and all associated interventions on animal welfare and the outcome of cancer monitoring studies. Therefore, we studied the potential impact of repeated native and contrast-enhanced (CE) CT imaging with 2 commonly used radiation doses on animal behavior, welfare, and breast cancer physiology as well as tumor therapy response.

MATERIAL AND METHODS

Animals

All animal experiments were approved by the State Office for Nature, Environment, and Consumer Protection (LANUV) in North Rhine-Westphalia, Germany.

Female BALB/cAnNRj mice (age 8–10 weeks; Janvier Labs, Saint Berthevin, France) were housed in groups of 5 in closed type II individually ventilated cages cages with a temperature of 20°C to 24°C, a humidity of 45% to 65%, and a 12-hour light/dark cycle, on spruce granulated bedding according to the guidelines of the Federation for Laboratory Animal Science Associations (www.felasa.eu). Food (Sniff GmbH, Soest, Germany) and water were accessible ad libitum. One nestlet per cage was provided to enable nest building. All efforts were made to minimize the number of animals used in this study and their suffering.

Orthotopic Tumor Inoculation and Antitumor Therapy

Tumor inoculation was performed 1 week before the first imaging session. For this purpose, murine triple-negative breast cancer cells (4T1,[30] ATCC CRL2539, Manassas, VA; 4×10^4 cells in 50 µL RPMI 1640 cell culture medium) were injected into the right mammary fat pad of 111 mice. The tumor sizes were measured daily with a caliper (Supplemental Digital Content, Fig. S5, http://links.lww.com/RLI/A775), and the tumor volumes were calculated [length × width × width × (π/6)]. Tumors with a volume of more than 5 mm^3 on day 6 after tumor cell inoculation were included in the analyses.

Animals were treated with the tyrosine kinase inhibitor regorafenib (therapy group) (Merck, Darmstadt, Germany) or vehicle solution (60 µL via oral gavage; control group). The vehicle solution consisted of 34% 1,2-propanediol, 34% polyethyleneglycol 400, and 0.12% pluronic F68 (Merck) in deionized water and provided the base for the therapy solution, which additionally contained regorafenib (Merck; 10 mg/kg body weight).[31]

Experimental Setup

The influence of repeated CT scans on animal welfare and tumor growth was investigated in the following experimental groups, consisting of at least 20 animals each: (1) no imaging (control), (2) isoflurane anesthesia, (3) 4 mGy CT, (4) 50 mGy CT, and (5) CE 50 mGy CT (CE-CT) (Fig. 1A). Animals were trained for the behavioral rotarod test and heart rate measurements on days −10, −8, −6, −4, and −2 and tumor cells were inoculated on day 0. Baseline measurements for rotarod and heart rate were performed on days 4 and 6. Half of the animals in each group were randomly selected to receive the daily antitumor therapy from day 6 on. Administration of anesthesia alone (30 minutes, 2% isoflurane in 98% O_2) or in combination with CT was performed on days 7, 10, and 14 after tumor cell injection, and rotarod performance and heart rate were evaluated on day 11, 13, and 15. Animals were sacrificed on day 15.

CT Protocol

Imaging was performed with the MILabs U-CTi CT-FLT combination device (MILabs, Houten, the Netherlands). Imaging with 4 mGy was conducted with the "total body–fast" scan protocol implemented in the system with the following parameters: 55 kV tube voltage, 0.17 mA tube current, 20 milliseconds exposure time, 40 degrees/s angle speed, 0 degree step angle, and 2 × 2 pixel binning with a total scan time of 19 seconds. Imaging with 50 mGy was performed with the "total body–normal" scan protocol with the following settings: 55 kV tube voltage, 0.17 mA tube current, 75 milliseconds exposure time, 0 degrees/s angle speed, 0.750 degrees step angle, and 1 × 1 pixel binning with a total scan time of 251 seconds (Figs. 1B, C). For CE scans, iomeprol (Imeron 400 M, Bracco, Italy, 400 mg/mL iodine) was injected intravenously with a dose of 2 mg/kg bodyweight in 0.9% NaCl.

Influence of Repeated Low-Dose CT on Animal Welfare

Animal welfare was evaluated daily with a score sheet,[32] which considered body weight, the animals' general condition, spontaneous behavior, and tumor growth. The point system ranged from 0 points (no alteration) to 20 points (humane endpoint) and was used as an indicator for animal health state (Supplemental Digital Content 1, Table 1 http://links.lww.com/RLI/A775). Scoring was performed blinded to the treatment group of the animal.

Motor coordination and balance were investigated by the rotarod performance test (Panlab Harvard Apparatus, Barcelona, Spain). Therefore, animals were placed on a rotating cylinder with accelerating speed, starting at 4 rotations per minute. After 5 minutes, a maximum speed of 40 rotations per minute could be reached and the time until mice fell off the cylinder was documented. Rotarod performance was indicated by the time each animal stayed on the cylinder. The animals were trained 5 times before the tumor cell injection and baseline values were acquired on days 4 and 6 after tumor inoculation. After the training phase, motor coordination measurements were performed on days 11, 13, and 15.

Subsequent to the rotarod test, heart rate measurements were performed using a CODA System (Kent Scientific Corporation, Torrington, CT) to evaluate discomfort and stress in the animals. After restraining the mice in a plexiglas tube, the heart rate was assessed with a tail volume pressure cuff and analyzed as described previously.[5]

Stress hormone levels were determined by fecal corticosterone metabolite (FCM) analysis.[33] Feces were collected during rotarod and heart rate measurements. After storing the samples at −80°C, they were dried at 60°C for at least 12 hours. Fifty milligrams of each sample were diluted overnight at 4°C in 500 µL of 80% methanol (Merck) and were homogenized afterward. After centrifugation (Fresco 21 and Pico 21; Heraeus, Hanau, Germany) for 10 minutes at 3000 rpm, an aliquot of the supernatant was analyzed with the 5α-pregnane-3β,11β,21-triol-20-one enzyme immunoassay.[26]

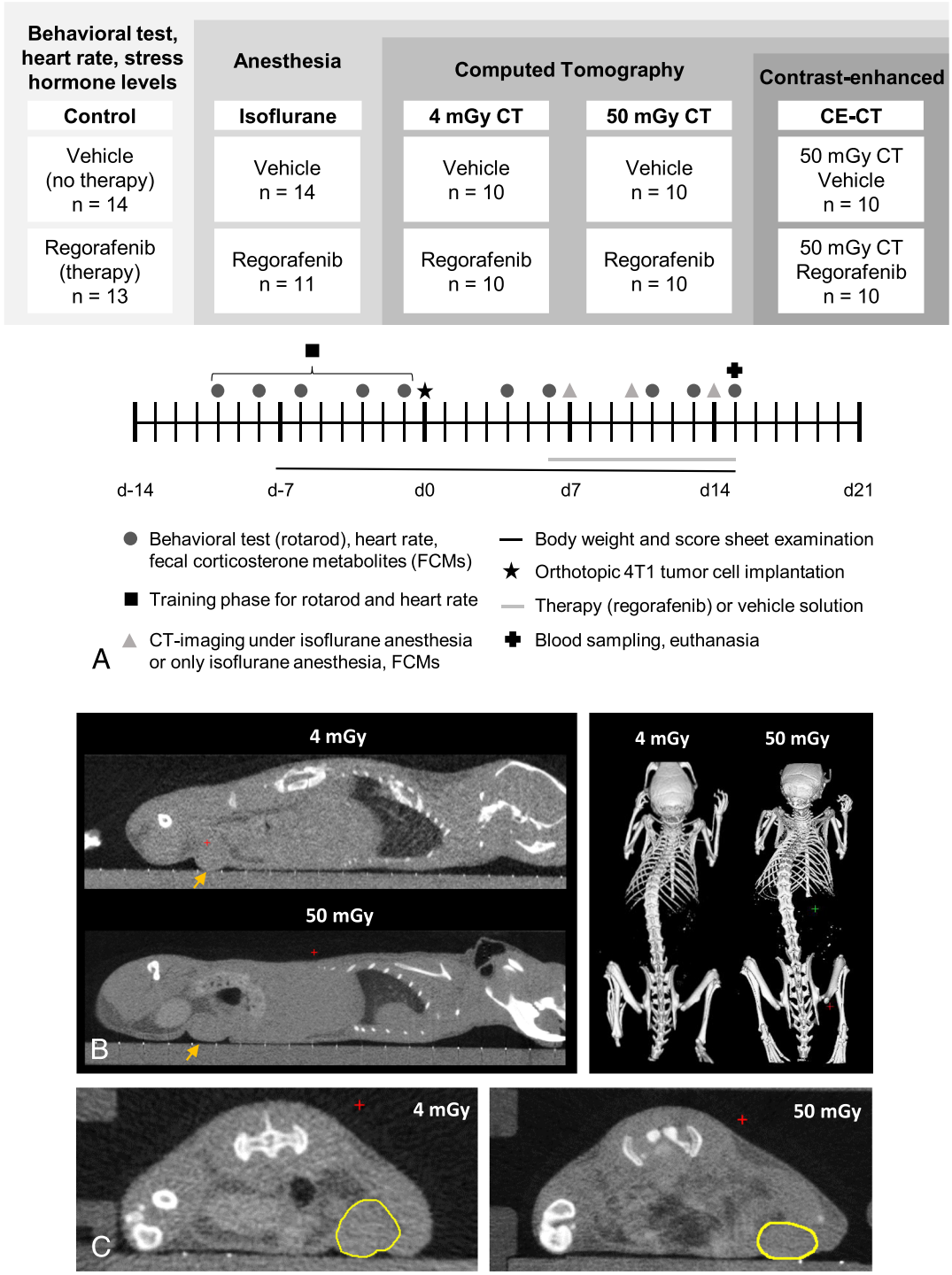

FIGURE 1. A, Groups and study design. All animals underwent a behavioral test (rotarod), heart rate measurements, and FCM analysis twice per week. Animals were trained for the behavioral test and heart rate measurements 5 times prior to the tumor cell implantation. Anesthesia-only groups and CT-imaged groups received isoflurane anesthesia for 20 minutes 3 times within 1 week. CT imaging was performed native at 4 and 50 mGy, and CE-CT scans were performed at 50 mGy with Imeron 400. B, Sagittal mouse images of 4 and 50 mGy CT scans, 4T1 tumors are indicated by an arrow. C, Axial images of 4 and 50 mGy CT scans of mice containing the 4T1 tumors (yellow circle).

For rotarod performance, heart rate measurements, and FCM analysis, mean baseline values were calculated from days 4 and 6 for each animal. Afterward, baseline values were set to 100% and the change in the subsequent measurements in comparison with the baseline was calculated. Group means were reported with standard deviation.

Hemograms

Blood samples were taken on the last day of the experiment by retrobulbar sinus puncture, and blood was stored for 30 minutes in heparin tubes at room temperature. After centrifugation at 3000 rpm for 10 minutes, hemograms (leukocytes, thrombocytes, hemoglobin, hematocrit, erythrocytes) were analyzed using a Celltac alpha MEK-6550 device (Nihon Kohden, Shinjuku, Japan).

Tumor Tissue Preparation

On the last day of the experiment, animals were intraperitoneally injected with ketamine/xylazine in 0.9% NaCl (120 mg/kg body weight ketamine/16 mg/kg body weight xylazine; 30 µL/10 g body weight), and mice were injected with rhodamine-labeled *Ricinus communis* agglutinin I (15 mg/kg body weight; Vector Laboratories, Burlingame, CA; intravenous injection into the tail vein) to stain perfused tumor vessels. Subsequently, heart perfusion was performed as described previously,[5] and organs (brain, heart, lungs, liver, spleen, and kidneys), as well as tumors, were removed. After a macroscopic inspection, organs and tumors were weighted and embedded in Tissue Tek O.C.T. Compound (Sakura, Alphen aan den Rijn, the Netherlands) for storage at −80°C.

Immunohistology

After cryosectioning tumors into 8-µm-thick sections (CM3050S, Leica, Wetzlar, Germany), the tissue was fixed with 4°C cold 80% methanol for 5 minutes (Merck) and ice-cold acetone for 2 minutes (Merck). For blood vessel density evaluation, the sections were stained with rat-antimouse PECAM-1 monoclonal CD31 (#553370; BD Bioscience, San Jose, CA) and donkey-antirat IgG (H + L) (#712-546-153; Dianova, Hamburg, Germany). Proliferating cells were stained with rabbit-antimouse polyclonal Ki67 (#ab15580; Abcam, Cambridge, UK), followed by donkey-antirabbit IgG (H + L) (#711-546-152; Dianova). Nuclei were stained with 4′,6-diamidino-2-phenylindole (DAPI [0.5 mg/mL]; Merck) in all tumor sections.

For each tumor, 5 micrographs per section, captured with an Axio imager M2 microscope (Zeiss, Göttingen, Germany) and a high-resolution camera (AxioCam MRm Rev.3; Zeiss, Göttingen, Germany), were analyzed with ImageJ2[34] and the image processing package Fiji (National Institutes of Health, Bethesda, MD). The CD31-positive area was colocalized with the rhodamine-labeled *R communis* agglutinin I–positive area fraction to determine the amount of perfused vessels. Proliferation was quantified by determining the area fraction of Ki67-positive cells in relation to all DAPI-positive cells.

Statistical Analysis

Statistical analysis was performed with GraphPad Prism 9 (Graphpad Software, v9.4.0, San Diego, CA, academic license). After testing for normal distribution, longitudinal data were analyzed with the repeated-measures analysis of variance and Tukey post hoc test. Data of the last experiment day were analyzed with 1-way analysis of variance and Tukey post hoc test with 95% confidence interval. P values <0.05 were considered to be statistically significant.

RESULTS

Influence of Repeated Native and CE-CT on Animal Welfare

Score Sheets

According to the score sheet evaluation (Fig. 2A, Table 1), overall animal burden was increasing throughout the experiment in all groups. This was caused by tumor growth and some animals in all groups exceeded the mild burden range to a medium range. Overall, anesthesia-receiving and CT-imaged animals showed higher scores at the end of the experiment than the control groups ($P < 0.001$, on the last day of the experiment).

Rotarod

The rotarod performance was not influenced by repeated native and CE-CT scans in untreated animals (Fig. 2B, Table 1) ($P = 0.269$, on the last day of the experiment). On the contrary, regorafenib-treated mice showed decreased rotarod performance when scanned with CE-CT in comparison with the control and isoflurane cohorts at the last day of the experiment (Fig. 2D, Table 1).

Heart Rate and FCMs

Repeated anesthesia, CT, and CE-CT showed no significant effect on the heart rate of untreated and treated animals of the various groups (Fig. 2C, Table 1) ($P = 0.185$, on the last day of the experiment). Stress hormone levels on the last day were compared with the baseline values and were not significantly influenced in imaged animals in comparison with the controls (Supplemental Digital Content 1, Fig. S2, http://links.lww.com/RLI/A775; Table 1).

Hemograms

Blood was taken on the last day of the experiments and its analysis indicated no alteration in the health of animals after repeated anesthesia, native and CE-CT scans, or tumor therapy administration according to leukocyte, erythrocyte, and thrombocyte counts as well as hemoglobin and hematocrit values (Supplemental Digital Content 1, Figs. S1A–E and Table S2, http://links.lww.com/RLI/A775).

Organ Weights

No significant differences in liver, heart, lung, kidney, and brain weights were found after repeated anesthesia, native and CE-CT scans, or tumor therapy administration. Spleen weights were slightly reduced in all nontreated animals that received isoflurane anesthesia (Supplemental Digital Content 1, Figs. S4A–E, http://links.lww.com/RLI/A775; Table 2). This effect was rendered statistically significant in the 4 mGy CT imaging group ($P = 0.003$).

Tumor Weight and Immunohistology

Overall, treated animals showed a lower tumor weight than nontreated animals on the last day of the experiment ($P = 0.041$, Fig. 3A; Supplemental Digital Content 1, Table S3, http://links.lww.com/RLI/A775), which was significant in the control and CE-CT groups. Neither anesthesia nor imaging had a measurable influence on the tumor weight.

The histological analysis revealed no alteration in tumor vessel density in nontreated ($P = 0.122$) and regorafenib-treated ($P = 0.386$) animals (Fig. 3B, Table 3). However, tumors showed a significantly higher percentage of perfused vessels after native 4 mGy and CE-CT scans in untreated animals and a significantly higher percentage of perfused vessels after 4 mGy imaging in regorafenib-treated animals in comparison with the control groups ($P < 0.001$) (Fig. 3C, Table 3). Overall, proliferating (Ki67-positive) cells were lower in regorafenib-treated animals. Furthermore, proliferation was reduced after repeated native and CE-CT scans with a significant effect in the nontreated CE-CT group ($P < 0.001$, Fig. 4, Table 3).

DISCUSSION

From an ethical point of view, it is crucial to reduce animal suffering during the experiments to an absolute minimum. Even though imaging modalities have been repeatedly described as safe,[35] the number and frequency of procedures, as well as the effects of anesthesia and contrast agent administration, must be considered in the overall picture. In our study, we demonstrated that CT imaging has no influence on the motor coordination of mice and did not decrease animal welfare significantly. However, if CT scans were combined with contrast agent injection and regorafenib therapy, the motor coordination of the animals was strongly affected. This became more pronounced with the repetition of

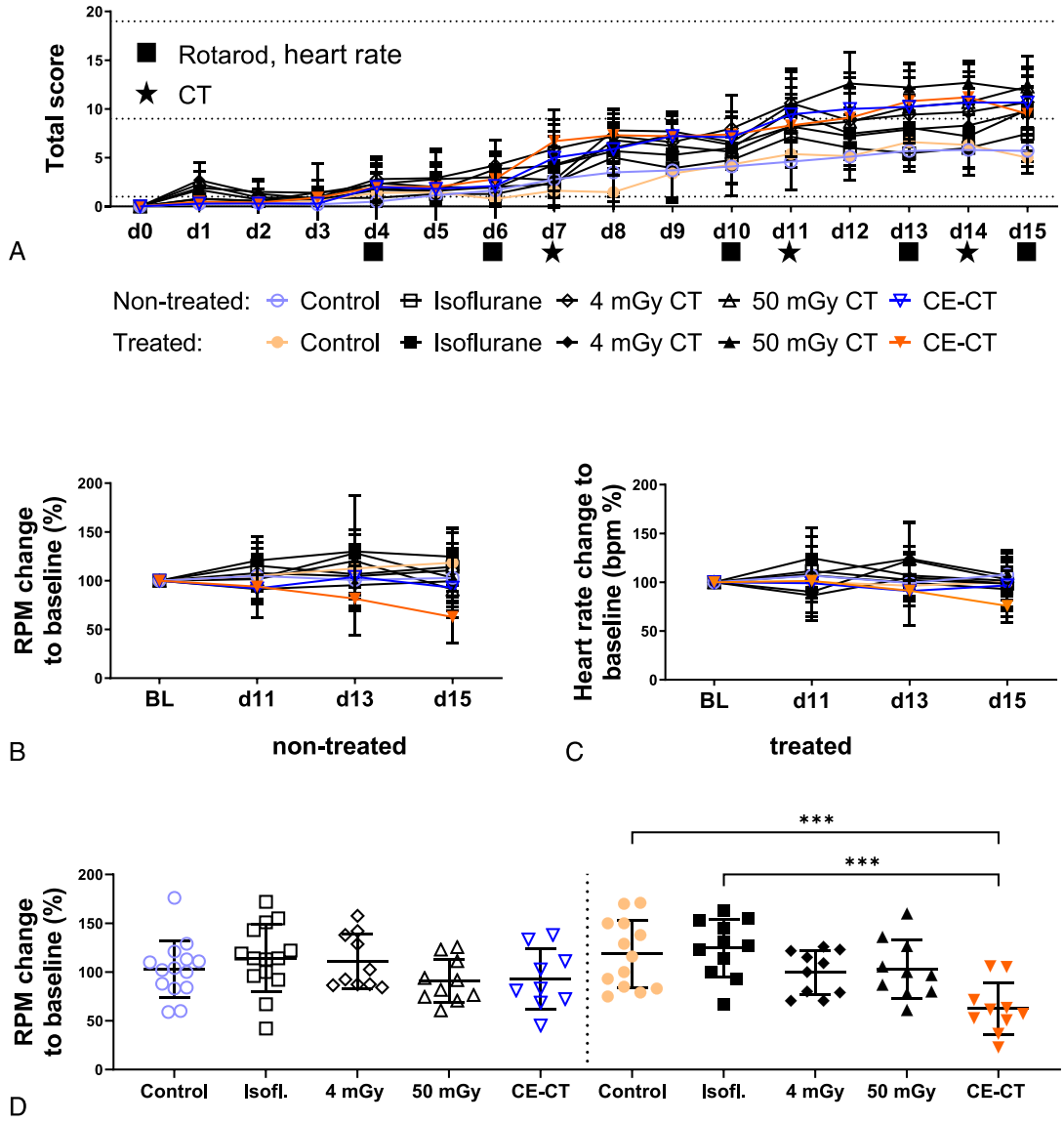

FIGURE 2. Animal welfare evaluation in 4T1 tumor–bearing BALB/c mice. BL indicates baseline. A, The score sheet evaluation shows a low to medium burden in all groups, which is related to the tumor growth. B, D, Rotarod performance is significantly decreased in animals after repeated CE-CT and therapy administration on the last day of the experiment. C, The heart rate is not significantly impaired by CT imaging. ***$P \leq 0.001$.

interventions. In contrast to the decreasing motor coordination, score sheets and the stress hormone levels were not significantly changed. In the score sheets, the motor coordination impairment of the CE-CT group might have been masked by the effects of tumor growth and anesthesia administration, which already increased the severity stage. However, although the score sheet is undoubtedly a valuable tool for tracking the degree of severity,[36] the motor coordination test might have been more sensitive. This assumption is strengthened by other studies, for example, on an amyotrophic lateral sclerosis mouse model, where the rotarod test was able to indicate changes in animal welfare 1 week prior to the general score sheet.[37]

Regarding inhalation anesthesia agents, isoflurane is among the most suitable ones for preclinical studies owing to its good controllability, high stability, low blood solubility, and little biodegradation.[38] Nevertheless, reports about adverse effects like neuroapoptosis[39,40] and possible DNA damage induction[41] have become more prominent in the past years. Similar side effects were observed for alternative inhalation agents, such as sevoflurane or desflurane in human cells.[42] Regarding physiological alterations, the spleen weight was reduced in all nontreated but anesthetized animals, compared with control animals (significant in the nontreated 4 mGy group). The spleen weight reduction was in line with a previous study where we demonstrated an imaging-independent, isoflurane-induced spleen weight reduction in healthy BALB/c mice.[5] However, the spleen weight reduction was less prominent in the 4T1 tumor–bearing animals in comparison with healthy animals. This can be explained by the influence of 4T1 tumor growth and regorafenib treatment on spleen size, which may have partially masked the isoflurane effect.[5] Potential alternatives to inhalation anesthetics are intravenous anesthesia agents such as ketamine or propofol. However, also these agents affect animal (patho-)physiology. For example, propofol was shown to have an antioxidative effect,[38] which can counteract antitumor therapies. Moreover, as inhalation anesthetics, ketamine and propofol can exert immunosuppressive effects.[43,44] In terms of administration, intravenous anesthetics might be countered by the ease of use and administration of

TABLE 1. Mean ± SD Values of the Score Sheet Analysis, Behavioral Test (Rotarod), Heart Rate, and FCM Measurements in Nontreated and Treated 4T1 Tumor–Bearing BALB/c Mice on the Last Day of the Experiment

Parameter	Control	Isoflurane	4 mGy CT	50 mGy CT	CE-CT
Nontreated					
Score (points)	5.7 ± 1.6	9.0 ± 5.5	10.7 ± 2.6	12.3 ± 3.1	10.7 ± 2.8
Rotarod, %	103 ± 30	114 ± 35	111 ± 28	91 ± 22	93 ± 31
Heart rate, %	108 ± 22	99 ± 34	103 ± 18	107 ± 17	97 ± 15
FCMs, %	108 ± 43	119 ± 54			114 ± 42
Regorafenib treated					
Score (points)	5.4 ± 0.5	9.9 ± 4.2	9.8 ± 2.4	11.9 ± 2.4	9.5 ± 2.9
Rotarod, %	118 ± 35	127 ± 30	100 ± 23	103 ± 30	63 ± 27
Heart rate, %	101 ± 26	93 ± 20	99 ± 17	102 ± 30	76 ± 17
FCMs, %	118 ± 50	128 ± 68			112 ± 31

Rotarod, heart rate, and FCM values are given as percentage change to the baseline.

FCM indicates fecal corticosterone metabolites; CT, computed tomography; CE, contrast enhanced.

inhalation anesthetics, which allow anesthesia to be delivered in a very precise manner without long recovery periods. In both cases, possible anesthesia side effects must be considered when evaluating study results.

As expected, the therapy with regorafenib led to a reduction in tumor weight, which can be mainly caused by immunogenic cell death induction[45] and inhibition of stromal interactions.[46] Even though tumor weights showed a high standard deviation, they were not influenced by our imaging interventions. This is in line with the literature, where a size reduction was described only for higher doses than used in our study. For instance, Moding et al[47] demonstrated a significantly reduced sarcoma growth after tumor radiation with 20 Gy. However, at doses between 500 mGy and 2 Gy ionizing radiation, there are also controversial reports about radiation-induced tumorigenesis,[48] which also did not apply to our case.

Going more into detail, we did not observe an alteration in the tumor blood vessel density caused by the imaging procedure. In line with our results, it was reported that radiation-induced damage in tumor vascularization usually only occurs at high radiation doses and goes along with increased HIF-1 levels and tumor hypoxia,[49] endothelial cell death, destruction of the microvasculature by p53 pathway activation, and a collapse of the blood vessels.[50] However, we detected an overall increase in the percentage of perfused tumor vessels after repeated CT imaging. This consistent trend was seen in all CT imaged groups but statistically significant results were obtained only for the nontreated 4 mGy and CE-CT and treated 4 mGy groups owing to high standard deviations. Similar findings, regarding an increased amount of perfused tumor vessels after radiation, were described by Crokart et al[51] in a C3H mouse liver cancer model after irradiation with 2 Gy. On the contrary, a reduction in tumor perfusion was found in syngeneic melanomas[52] and human colon cancer xenografts[53] in mice after radiotherapy with 12 Gy. These effects may depend on the time point of perfusion assessment and the applied radiation dose. In a human laryngeal squamous cell carcinoma xenograft model, Bussink and colleagues[54] reported an initial increase in vascular perfusion after irradiation with 10 Gy, which changed to a decrease after 26 hours after irradiation and normalized after 7 days.

Increased perfusion at stable vessel density might be explained by the opening of nonfunctional vessels, which comprise a significant portion of malignant tumors, owing to radiation-induced vascular decompression. This hypothesis is supported by our finding that tumor cell proliferation was slightly decreased after CT imaging, especially

TABLE 2. Mean ± SD Organ Weights of Untreated and Treated 4T1 Tumor–Bearing Mice After Repeated CT Imaging on the Last Day of the Experiment

Organ (g)	Control	Isoflurane	4 mGy CT	50 mGy CT	CE-CT
Nontreated					
Kidneys	0.282 ± 0.04	0.270 ± 0.03	0.254 ± 0.03	0.267 ± 0.03	0.267 ± 0.02
Heart	0.121 ± 0.02	0.115 ± 0.02	0.123 ± 0.02	0.122 ± 0.01	0.125 ± 0.01
Lung	0.203 ± 0.05	0.191 ± 0.03	0.174 ± 0.06	0.206 ± 0.06	0.026 ± 0.08
Brain	0.414 ± 0.03	0.406 ± 0.02	0.432 ± 0.02	0.421 ± 0.02	0.432 ± 0.02
Liver	1.085 ± 0.17	0.937 ± 0.14	0.905 ± 0.09	1.105 ± 0.17	1.027 ± 0.07
Spleen	0.288 ± 0.08	0.252 ± 0.05	0.205 ± 0.06	0.237 ± 0.09	0.232 ± 0.05
Regorafenib treated					
Kidneys	0.271 ± 0.04	0.279 ± 0.03	0.249 ± 0.02	0.263 ± 0.03	0.270 ± 0.02
Heart	0.115 ± 0.02	0.119 ± 0.02	0.116 ± 0.01	0.117 ± 0.02	0.117 ± 0.01
Lung	0.201 ± 0.07	0.197 ± 0.04	0.181 ± 0.05	0.216 ± 0.05	0.237 ± 0.08
Brain	0.412 ± 0.03	0.407 ± 0.03	0.428 ± 0.02	0.418 ± 0.01	0.435 ± 0.02
Liver	1.003 ± 0.10	0.954 ± 0.19	0.856 ± 0.09	1.033 ± 0.16	1.018 ± 0.15
Spleen	0.220 ± 0.06	0.236 ± 0.05	0.176 ± 0.04	0.231 ± 0.04	0.235 ± 0.03

CT indicates computed tomography; CE, contrast enhanced.

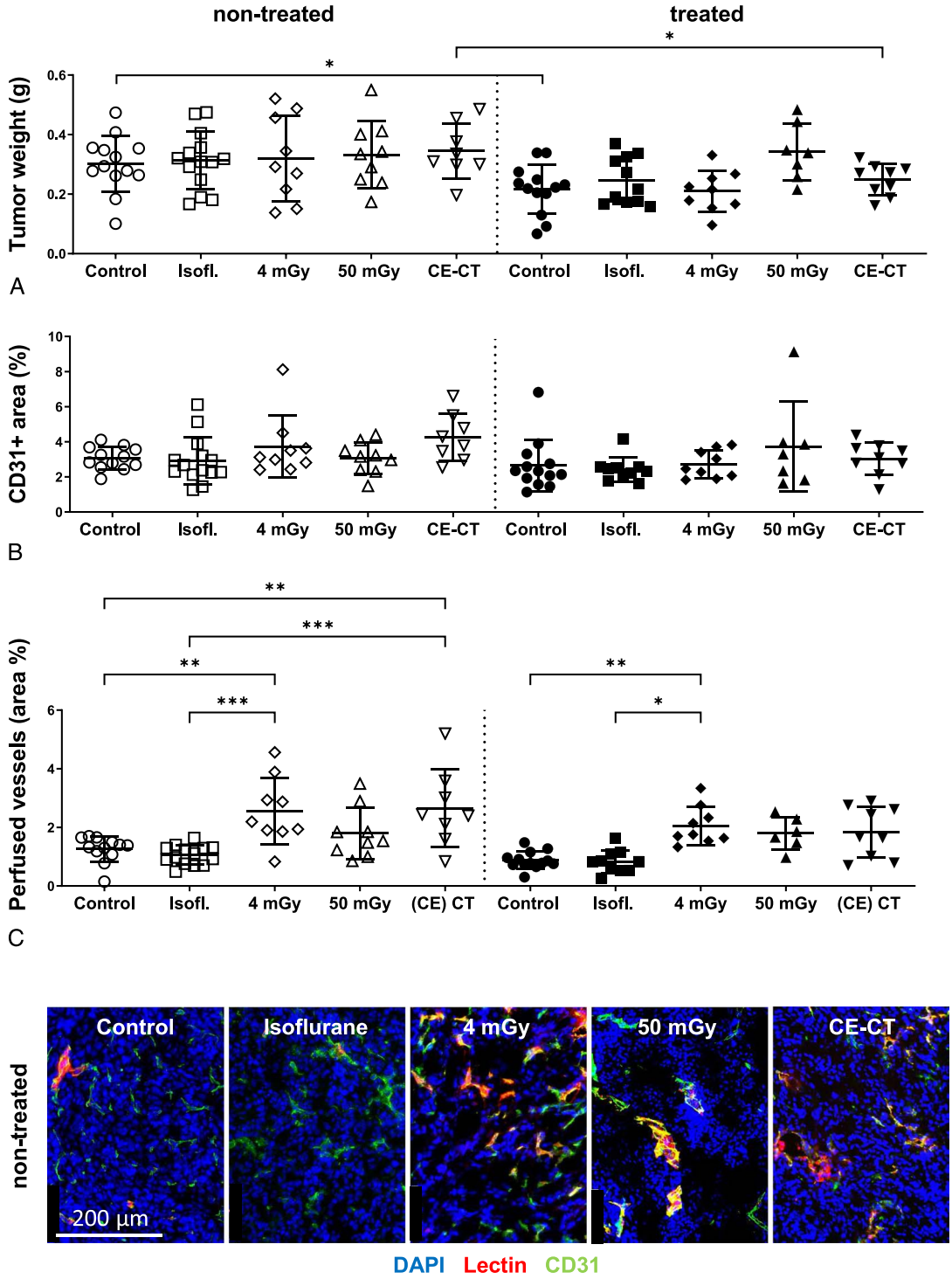

FIGURE 3. 4T1 tumor physiology after repeated native and CE-CT imaging. A, Tumor weights are lower in regorafenib-treated mice but not influenced by imaging or anesthesia. B, Tumor vessel density is not influenced by imaging or therapy administration. C, The percentage of perfused tumor vessels is higher in animals after repeated CT imaging independently of contrast agent application. Scale bar: 200 µm (images taken at ×20 magnification). $*P \leq 0.05$, $**P \leq 0.01$, $***P \leq 0.001$.

in nontreated animals. This can lead to reduced interstitial tumor pressure and, therefore, higher vessel perfusion. The radiation effect from CT was enhanced by the administration of the iodine-based contrast agent iomeprol, resulting in further inhibition of tumor cell proliferation. As described in a previous study, iodinated contrast agents can lead to a downregulation of the mechanistic target of rapamycin and extracellular signal-regulated kinase pathways, both mainly involved in proliferation regulation.[55]

The hypothesis of imaging-induced vascular decompression is further supported by our finding that the (CE-) CT-induced increase in

TABLE 3. Mean ± SD Percentage of Tumor Vessel Density (CD31+ Area Fraction) and Cell Proliferation (Ki67+ Area Fraction) in Untreated and Treated 4T1 Tumor–Bearing Mice After Repeated CT Imaging on the Last Day of the Experiment

Parameter	Control	Isoflurane	4 mGy CT	50 mGy CT	CE-CT
Nontreated					
Vessel density	3.06 ± 0.65	2.93 ± 1.34	3.73 ± 1.77	3.06 ± 0.91	4.25 ± 1.35
Perfused vessels	1.26 ± 0.44	1.05 ± 0.33	2.55 ± 1.14	1.80 ± 0.87	2.65 ± 1.33
Cell proliferation	27.61 ± 8.97	28.6 ± 13.45	21.61 ± 10.99	20.39 ± 8.39	12.00 ± 3.48
Regorafenib treated					
Vessel density	2.64 ± 1.46	2.44 ± 0.70	2.73 ± 0.79	3.72 ± 2.56	3.06 ± 0.93
Perfused vessels	0.88 ± 0.30	0.83 ± 0.39	2.06 ± 0.65	1.80 ± 0.56	1.84 ± 0.87
Cell proliferation	11.39 ± 3.66	15.36 ± 5.28	5.60 ± 2.20	4.37 ± 2.23	3.29 ± 1.57

The percentage of perfused vessels was determined by area fraction of rhodamine-labeled *Ricinus communis* agglutinin I–positive area fraction in relation to CD31+ area.

CT indicates computed tomography; CE, contrast enhanced.

the amount of perfused vessels and decrease in proliferating cells were less pronounced under regorafenib therapy, as the latter already induced a strong vascular decompression effect and proliferation inhibition,[31] thus masking the effect from CT imaging.

In addition, perivascular coverage of the vessels might also play a major role in tumor blood vessel physiology. Pericyte recruitment was shown to be increased after radiotherapy in the literature.[56] As pericytes are involved in blood flow regulation and tissue homeostasis, they may stabilize vessels leading to increased perfusion.[57] A similar effect was described previously by Potiron et al in an orthotopic prostate cancer model. The authors demonstrated a higher amount of perfused vessels along with overall vessel maturation and reduced tumor cell proliferation after radiotherapy. However, significantly higher radiation dose fractions of 2 Gy were applied over 2 weeks.[58]

A limitation of our study is the use of just 1 mouse strain, since radiation effects can depend significantly on the strain.[20,59] BALB/c mice were chosen as we intended to explore the effects of CT imaging on an immunocompetent tumor model. Further studies should be conducted in different strains and immunodeficient mice with tumor xenografts. Furthermore, behavioral and physiological alterations as well as radiosensitivity[60,61] can highly depend on animal sex. Nevertheless, because our study focused on breast cancers, female animals were the rational choice.

Concerning behavioral investigations, the Rotarod test is one of the most reliable tests for motor coordination, strength, and balance testing and can detect even small changes in this regard.[62] However, future studies could also include a focus on exploratory behavior and anxiety. Here, the open-field or maze tests might be appropriate. In addition, the possible influence of the iodine contrast agent on physiological parameters like liver enzymes could be examined.

Regarding the image quality acquired with our CT protocols, we observed that the 50 mGy scan protocol resulted in higher image quality

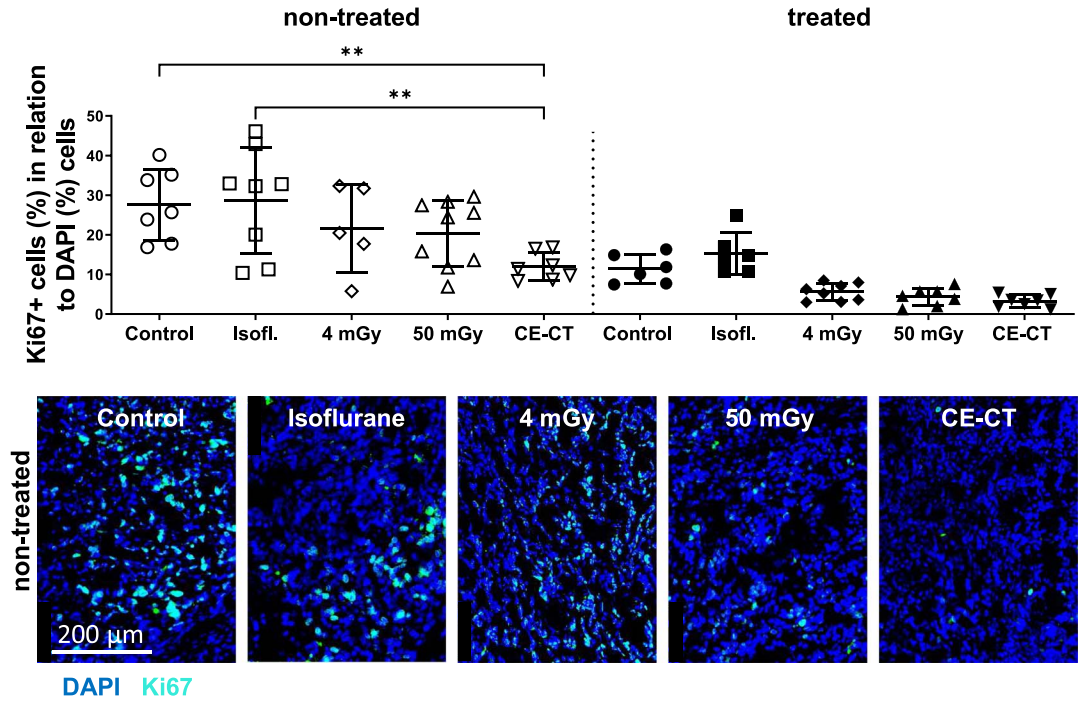

FIGURE 4. Tumor proliferation after repeated CT imaging. Tumor proliferation is slightly decreased in CT-imaged animals and significantly lower in nontreated animals after CE-CT. Scale bar: 200 µm (images taken at ×20 magnification). $^{**}P \leq 0.01$.

with less noise and better contrast than the 4 mGy one, which is in line with the literature describing improved image quality with increasing radiation dose.[63] However, orthotopic 4T1 tumors could be segmented in all cases. Considering that lower doses are always preferable from a biological and safety point of view, 4 mGy scans seem to be sufficient for tumor analysis. If the aim of the CT scan is restricted to tumor and organ segmentation, even lower x-ray doses could be evaluated.

In summary, we investigated the impact of native and CE-CT on animal welfare and 4T1 tumor physiology. Our results suggest that not the imaging itself but the combination of different interventions related to imaging may lead to a significant impairment of animal welfare, as indicated by the motor coordination reduction. Moreover, we could reveal a possible sensitivity limitation of the scoring system for animal welfare observations. Furthermore, we provide evidence that even low doses of radiation, outside of the radiotherapeutic range, may be capable of altering tumor perfusion significantly. This effect should be carefully considered when using CT as a diagnostic tool in preclinical oncological research and should be part of future investigations addressing the possible impact of imaging on animal welfare and study results.

REFERENCES

1. Russel WMS, Burch RL. *The Principles of Humane Experimental Technique: Preface*. Wheathampstead, United Kingdom: Universities Federation for Animal Welfare; 1959.
2. Tremoleda JL, Sosabowski J. Imaging technologies and basic considerations for welfare of laboratory rodents. *Lab Anim*. 2015;44:97–105.
3. Fischman AJ, Alpert NM, Rubin RH. Pharmacokinetic imaging: a noninvasive method for determining drug distribution and action. *Clin Pharmacokinet*. 2002; 41:581–602.
4. Beckmann N, Ledermann B. Noninvasive small rodent imaging: significance for the 3R principles. In: Kiessling F, Pichler BJ, Hauff P, eds. *Small Animal Imaging: Basics and Practical Guide*. Cham, Switzerland: Springer International Publishing; 2017:69–87.
5. Baier J, Rix A, Drude NI, et al. Influence of MRI examinations on animal welfare and study results. *Invest Radiol*. 2020;55:507–514.
6. Girbig RM, Baier J, Palme R, et al. Welfare assessment on healthy and tumor-bearing mice after repeated ultrasound imaging. *Eur Surg Res*. 2022;1–12.
7. Pasquini L, Napolitano A, Visconti E, et al. Gadolinium-based contrast agent–related toxicities. *CNS Drugs*. 2018;32:229–240.
8. Shahid I, Lancelot E, Desché P. Future of diagnostic computed tomography: an update on physicochemical properties, safety, and development of x-ray contrast media. *Invest Radiol*. 2020;55:598–600.
9. Hasebroock KM, Serkova NJ. Toxicity of MRI and CT contrast agents. *Expert Opin Drug Metab Toxicol*. 2009;5:403–416.
10. Mannheim JG, Schlichthaerle T, Kuebler L, et al. Comparison of small animal CT contrast agents. *Contrast Media Mol Imaging*. 2016;11:272–284.
11. Deinzer CKW, Danova D, Kleb B, et al. Influence of different iodinated contrast media on the induction of DNA double-strand breaks after in vitro x-ray irradiation. *Contrast Media Mol Imaging*. 2014;9:259–267.
12. Gargiulo S, Greco A, Gramanzini M, et al. Mice anesthesia, analgesia, and care, part I: anesthetic considerations in preclinical research. *ILAR J*. 2012;53:E55–E69.
13. Jacobsen KO, Villa V, Miner VL, et al. Effects of anesthesia and vehicle injection on circulating blood elements in C3H/HeN male mice. *Contemp Top Lab Anim Sci*. 2004;43:8–12.
14. Stollings LM, Jia L-J, Tang P, et al. Immune modulation by volatile anesthetics. *Anesthesiology*. 2016;125:399–411.
15. Hurst JL, West RS. Taming anxiety in laboratory mice. *Nat Methods*. 2010;7: 825–826.
16. Wilde E, Aubdool AA, Thakore P, et al. Tail-cuff technique and its influence on central blood pressure in the mouse. *J Am Heart Assoc*. 2017;6:e005204.
17. Gu H, Tang C, Yang Y. Psychological stress, immune response, and atherosclerosis. *Atherosclerosis*. 2012;223:69–77.
18. Grunz JP, Petritsch B, Luetkens KS, et al. Ultra-low-dose photon-counting CT imaging of the paranasal sinus with tin prefiltration: how low can we go? *Invest Radiol*. 2022;57:728–733.
19. Raman SP, Johnson PT, Deshmukh S, et al. CT dose reduction applications: available tools on the latest generation of CT scanners. *J Am Coll Radiol*. 2013;10: 37–41.
20. Homolka P, Leithner R, Billinger J, et al. Ergebnisse der Österreichischen CT-Dosisstudie 2010: Effektive Dosen der häufigsten CT-Untersuchungen und Unterschiede zwischen Anwendern. *Z Für Med Phys*. 2014;24:224–230.
21. Tang FR, Loke WK, Khoo BC. Low-dose or low-dose-rate ionizing radiation-induced bioeffects in animal models. *J Radiat Res*. 2017;58:165–182.
22. Callahan MJ, MacDougall RD, Bixby SD, et al. Ionizing radiation from computed tomography versus anesthesia for magnetic resonance imaging in infants and children: patient safety considerations. *Pediatr Radiol*. 2018;48:21–30.
23. Tonolini M, Valconi E, Vanzulli A, et al. Radiation overexposure from repeated CT scans in young adults with acute abdominal pain. *Emerg Radiol*. 2018;25:21–27.
24. Pecaut MJ, Haerich P, Zuccarelli Miller CN, et al. The effects of low-dose, high-LET radiation exposure on three models of behavior in C57BL/6 mice. *Radiat Res*. 2004;162:148–156.
25. Giarola RS, De Almeida GHO, Hungaro TH, et al. Low-dose ionizing radiation exposure during pregnancy induces behavioral impairment and lower weight gain in adult rats. Arxiv, Biological Physics, Cornell University; 2019.
26. Kovalchuk A, Mychasiuk R, Muhammad A, et al. Liver irradiation causes distal bystander effects in the rat brain and affects animal behaviour. *Oncotarget*. 2016;7:4385–4398.
27. Poojary R, Kumar NA, Kumarchandra R, et al. Cynodon dactylon extract ameliorates cognitive functions and cerebellar oxidative stress in whole body irradiated mice. *Asian Pac J Trop Biomed*. 2019;9:278.
28. MacCallum DE, Hall PA, Wright EG. The Trp53 pathway is induced in vivo by low doses of gamma radiation. *Radiat Res*. 2001;156:324–327.
29. Yu H-S, Liu Z-M, Yu X-Y, et al. Low-dose radiation induces antitumor effects and erythrocyte system hormesis. *Asian Pac J Cancer Prev*. 2013;14:4121–4126.
30. Aslakson CJ, Miller FR. Selective events in the metastatic process defined by analysis of the sequential dissemination of subpopulations of a mouse mammary tumor. *Cancer Res*. 1992;52:1399–1405.
31. Wilhelm SM, Dumas J, Adnane L, et al. Regorafenib (BAY 73-4506): a new oral multikinase inhibitor of angiogenic, stromal and oncogenic receptor tyrosine kinases with potent preclinical antitumor activity. *Int J Cancer*. 2011;129:245–255.
32. Kanzler S, Rix A, Czigany Z, et al. Recommendation for severity assessment following liver resection and liver transplantation in rats: part I. *Lab Anim*. 2016;50: 459–467.
33. Palme R. Non-invasive measurement of glucocorticoids: advances and problems. *Physiol Behav*. 2019;199:229–243.
34. Rueden CT, Schindelin J, Hiner MC, et al. ImageJ2: ImageJ for the next generation of scientific image data. *BMC Bioinformatics*. 2017;18:529.
35. Liu C-N, Morin J, Dokmanovich M, et al. Nanoparticle contrast-enhanced micro-CT: a preclinical tool for the 3D imaging of liver and spleen in longitudinal mouse studies. *J Pharmacol Toxicol Methods*. 2019;96:67–77.
36. Bugnon P, Heimann M, Thallmair M. What the literature tells us about score sheet design. *Lab Anim*. 2016;50:414–417.
37. Knippenberg S, Thau N, Dengler R, et al. Significance of behavioural tests in a transgenic mouse model of amyotrophic lateral sclerosis (ALS). *Behav Brain Res*. 2010;213:82–87.
38. Senoner T, Velik-Salchner C, Luckner G, et al. Anesthesia-induced oxidative stress: are there differences between intravenous and inhaled anesthetics? *Oxid Med Cell Longev*. 2021;2021:8782387.
39. Johnson SA, Young C, Olney JW. Isoflurane-induced neuroapoptosis in the developing brain of nonhypoglycemic mice. *J Neurosurg Anesthesiol*. 2008;20:21–28.
40. Xie Z, Dong Y, Maeda U, et al. The common inhalation anesthetic isoflurane induces apoptosis and increases amyloid β protein levels. *Anesthesiology*. 2006;104:988–994.
41. Ni C, Li C, Dong Y, et al. Anesthetic isoflurane induces DNA damage through oxidative stress and p53 pathway. *Mol Neurobiol*. 2017;54:3591–3605.
42. Cukurova Z, Cetingok H, Ozturk S, et al. DNA damage effects of inhalation anesthetics in human bronchoalveolar cells. *Medicine (Baltimore)*. 2019;98:e16518.
43. Liu FL, Chen TL, Chen RM. Mechanisms of ketamine-induced immunosuppression. *Acta Anaesthesiol Taiwan*. 2012;50:172–177.
44. Yamaguchi A, Kawagoe I, Inoue S, et al. Propofol decreases CD8+ T cells and sevoflurane increases regulatory T cells after lung cancer resection: a randomized controlled trial. *J Thorac Dis*. 2021;13:5430–5438.
45. Liu CY, Lau KY, Huang TT, et al. Abstract P3-05-19: regorafenib induces immunogenic cell death via p-stat3 inhibition in triple negative breast cancer cells. *Cancer Res*. 2018;78(4_suppl):3–05–3–19.
46. Zopf D, Scholz A, Fichtner I, et al. Abstract 4262: Regorafenib (BAY 73-4506): a broad spectrum tumor deactivator with high combinability potential and antimetastasis activity. *Cancer Res*. 2011;71(8_suppl):4262.
47. Moding EJ, Clark DP, Qi Y, et al. Dual-energy micro-computed tomography imaging of radiation-induced vascular changes in primary mouse sarcomas. *Int J Radiat Oncol Biol Phys*. 2013;85:1353–1359.
48. Sofia Vala I, Martins LR, Imaizumi N, et al. Low doses of ionizing radiation promote tumor growth and metastasis by enhancing angiogenesis. *PLoS ONE*. 2010;5:e11222.
49. Brown JM. Radiation damage to tumor vasculature initiates a program that promotes tumor recurrences. *Int J Radiat Oncol Biol Phys*. 2020;108:734–744.

50. Park HJ, Griffin RJ, Hui S, et al. Radiation-induced vascular damage in tumors: implications of vascular damage in ablative hypofractionated radiotherapy (SBRT and SRS). *Radiat Res*. 2012;177:311–327.
51. Crokart N, Jordan BF, Baudelet C, et al. Early reoxygenation in tumors after irradiation: determining factors and consequences for radiotherapy regimens using daily multiple fractions. *Int J Radiat Oncol Biol Phys*. 2005;63:901–910.
52. Tsai JH, Makonnen S, Feldman M, et al. Ionizing radiation inhibits tumor neovascularization by inducing ineffective angiogenesis. *Cancer Biol Ther*. 2005;4:1395–1400.
53. Ren Y, Fleischmann D, Foygel K, et al. Antiangiogenic and radiation therapy: early effects on in vivo computed tomography perfusion parameters in human colon cancer xenografts in mice. *Invest Radiol*. 2012;47:25–32.
54. Bussink J, Kaanders JHAM, Rijken PFJW, et al. Changes in blood perfusion and hypoxia after irradiation of a human squamous cell carcinoma xenograft tumor line. *Radiat Res*. 2000;153:398–404.
55. Fernandes J, Abreu J. Iodinated contrast agents and their potential for antitumor chemotherapy. *Curr Top Biochem Res*. 2022;22:119–137.
56. Lan J, Wan XL, Deng L, et al. Ablative hypofractionated radiotherapy normalizes tumor vasculature in Lewis lung carcinoma mice model. *Radiat Res*. 2013;179:458–464.
57. Clément-Colmou K, Potiron V, Pietri M, et al. Influence of radiotherapy fractionation schedule on the tumor vascular microenvironment in prostate and lung cancer models. *Cancer*. 2020;12:121.
58. Potiron VA, Abderrahmani R, Clément-Colmou K, et al. Improved functionality of the vasculature during conventionally fractionated radiation therapy of prostate cancer. *PLoS ONE*. 2013;8:e84076.
59. Snijders AM, Marchetti F, Bhatnagar S, et al. Genetic differences in transcript responses to low-dose ionizing radiation identify tissue functions associated with breast cancer susceptibility. *PLoS ONE*. 2012;7:e45394.
60. Hultborn R, Albertsson P, Ottosson S, et al. Radiosensitivity: gender and order of administration of G-CSF, an experimental study in mice. *Radiat Res*. 2019;191:335–341.
61. Narendran N, Luzhna L, Kovalchuk O. Sex difference of radiation response in occupational and accidental exposure. *Front Genet*. 2019;10:260.
62. Oliván S, Calvo AC, Rando A, et al. Comparative study of behavioural tests in the SOD1G93A mouse model of amyotrophic lateral sclerosis. *Exp Anim*. 2015;64:147–153.
63. Goldman LW. Principles of CT: radiation dose and image quality. *J Nucl Med Technol*. 2007;35:213–225.